Physica E: Low-dimensional Systems and Nanostructures

Nonlocal free vibration characteristics of power-law and sigmoid functionally graded nanoplates considering variable nonlocal parameter

--Manuscript Draft--

Manuscript Number:	PHYSE-D-21-00274R1
Article Type:	Research Paper
Keywords:	Functionally graded materials; nanoplates; nonlocal elasticity theory; variable nonlocal parameter; free vibration.
Corresponding Author:	Vinh Văn Phạm Le Quy Don Technical University Hanoi, VIET NAM
First Author:	Vinh Văn Phạm
Order of Authors:	Vinh Văn Phạm
Abstract:	In this study, the effects of the variable nonlocal parameters on the free vibration of power-law and sigmoid functionally graded nanoplates are investigated using a simple inverse hyperbolic shear deformation theory incorporating with nonlocal elasticity theory. The novelty of this study is that the nonlocal parameter is assumed to vary smoothly through the thickness of the functionally graded nanoplates. The governing equations of motion are established using the variation form of Hamilton's principle, and they are solved via Navier's closed-form solution. Some verification studies are carried out to demonstrate the accuracy and efficiency of the proposed algorithm in predicting the free vibration behavior of functionally graded nanoplates. The effects of some parameters such as the aspect ratio, the side-to-thickness ratio, the power-law index as well as the variation of the nonlocal parameters are also considered carefully. The results show that the variation of the nonlocal parameter plays significant effects on the free vibration response of the functionally graded nanoplates. The influence of the nonlocal parameters on the free vibration of various kinds of functionally graded nanoplates is completely different, it depends on the variation of the material ingredients across the thickness of the functionally graded nanoplates.
Suggested Reviewers:	Mohammed Sobhy Kafrelsheikh University msobhy@sci.kfs.edu.eg His research interests lie in the areas of FGMs, micro/nanostructures and applied mathematics.
	Abdelouahed Tounsi University of Technology, Algeria abdelouahed.tounsi@univ-sba.dz His research interests lie in the areas of FGMs, micro/nanostructures.
	Ashraf M Zenkour Kafrelsheikh University zenkour@sci.kfs.edu.eg His research interests lie in the areas of FGMs, micro/nanostructures.
Response to Reviewers:	

Declaration of interests

☒The authors declare that they have no known competing financial interests or personal relationships that could have appeared to influence the work reported in this paper.

☐The authors declare the following financial interests/personal relationships which may be considered as potential competing interests:

HIGHLIGHTS

- A simple HSDT with a new inverse hyperbolic shape function is established.
- Nonlocal elasticity theory is modified with the vairable nonlocal parameter.
- The nonlocal parameter varies through the thickness of the FGM nanoplates.
- A comprehensive parameter study has been carried out carefully.

Nonlocal free vibration characteristics of power-law and sigmoid functionally graded nanoplates considering variable nonlocal parameter

Pham Van Vinh[1*]

[1] Department of Solid Mechanics, Le Quy Don Technical University, 236 Hoang Quoc Viet Street, Hanoi, Vietnam

Corresponding author: Pham Van Vinh (phamvanvinh@lqdtu.edu.vn)

Abstract:

In this study, the effects of the variable nonlocal parameters on the free vibration of power-law and sigmoid functionally graded nanoplates are investigated using a simple inverse hyperbolic shear deformation theory incorporating with nonlocal elasticity theory. The novelty of this study is that the nonlocal parameter is assumed to vary smoothly through the thickness of the functionally graded nanoplates. The governing equations of motion are established using the variation form of Hamilton's principle, and they are solved via Navier's closed-form solution. Some verification studies are carried out to demonstrate the accuracy and efficiency of the proposed algorithm in predicting the free vibration behavior of functionally graded nanoplates. The effects of some parameters such as the aspect ratio, the side-to-thickness ratio, the power-law index as well as the variation of the nonlocal parameters are also considered carefully. The results show that the variation of the nonlocal parameter plays significant effects on the free vibration response of the functionally graded nanoplates. The influence of the nonlocal parameters on the free vibration of various kinds of functionally graded nanoplates is completely different, it depends on the variation of the material ingredients across the thickness of the functionally graded nanoplates.

Keywords: Functionally graded materials; nanoplates; nonlocal elasticity theory; variable nonlocal parameter; free vibration.

1. Introduction

The investigation of micro/nanostructures is completely different from that of macro structures due to the small-scale effects. Therefore, the application of the classical continuum theory to study these structures can lead to erroneous results. To address this drawback, molecular dynamics (MD) can be served as an excellent method to predict the exact behavior of the micro/nanostructures, but the MD usually costs expensive computation. So, many higher-order continuum theories have been developed to analyze these structures. For example, the nonlocal elasticity theory [1-4], couple stress theory and modified couple stress theory [5-9], strain gradient theory and nonlocal strain gradient theory [10-16] have been introduced. The readers can get more information about these theories from the two review studies of Thai et al. [17] and Farajpour et al. [18].

The nonlocal elasticity theory, which is first established by Eringen, is usually used in combination with shear deformation theories by many scientists to analyze nanoplates, nanobeams and nanoshells. This nonlocal elasticity theory has been applied to analyze the mechanical and thermal behavior of micro/nanostructures made of isotropic homogeneous and heterogeneous materials. Functionally graded materials (FGMs) have many advantages in comparison with traditional materials, for instance, high performance, the resistance of high temperatures, etc. Therefore, the FGMs are also applied to produce micro/nanostructures in many fields of engineering and industry. More information about the fabrication, applications and analysis can be read from some researches of Tahir and Tounsi et al. [19-26], Vinh et al. [27-32] and their references. In the case of micro/nanostructures, Zhang et al. [33] applied nonlocal elasticity theory and classical shell theory to analyze buckling of multiwalled carbon nanotubes subjected to axial compressed load. Hu et al. [34] analyzed wave propagation in single-walled and double-walled carbon nanotubes via a combination of classical shell theory and nonlocal elasticity theory. Bellal et al. [35] studied buckling behavior of a single-layered graphene sheet resting on viscoelastic medium using a nonlocal four-unknown integral theory. Hussain et al. [36] employed nonlocal elasticity theory to analyze free vibration of armchair and zigzag single-walled carbon nanotubes. Asghar et al. [37] analyzed nonlocal frequencies of double-walled carbon nanotubes using nonlocal elasticity theory. Li et al. [38] studied vibration characteristics of multiwalled carbon nanotubes embedded in elastic media by a nonlocal elastic shell model. Wang et al. [39] applied a nonlocal elastic shell theory to analyze wave propagation of carbon nanotubes. Rouhi et al. [40] employed a nonlocal Flugge shell model to investigate axial buckling of double-walled carbon nanotubes with different end conditions. Matouk et al. [41] applied an integral Timoshenko beam theory to analyze the hygro-thermal vibration of FG nanobeams. Lu et al. [42] used first-order shear deformation theory (FSDT) in cooperating with nonlocal elasticity theory to analyze isotropic nanoplates. The small-scale effects on the vibration of embedded multilayered graphene sheets were investigated by Pradhan et al. [43] via nonlocal continuum models. Aksencer et al. [44] developed a Levy type solution for vibration and buckling analysis of nanoplates using nonlocal elasticity theory. The vibration of single-layered graphene sheet-based nanomechanical sensor was investigated by Shen et al. [45] via nonlocal Kirchhoff plate theory. A nonlocal continuum model based on Eringen nonlocal elasticity theory and classical plate theory has been developed by Zhang et al. [46,47]. In which, the kp-Ritz method has been employed as an element-free computational framework to analyze vibration and buckling behaviors of single-layered graphene sheets. Ansari et al. [48,49] analyzed the vibration of single-layered and multi-layered graphene sheets via Reissner-Mindlin theory and nonlocal elasticity theory. Hosseini-Hashemi [50] established an exact analytical solution based on nonlocal elasticity theory and FSDT for free vibration analysis of functionally graded (FG) circular/annular Mindlin nanoplates. Anjomshoa [51] developed a continuum model based on the FSDT and the nonlocal elasticity theory for free vibration analysis of embedded orthotropic thick circular and elliptical nano-plates resting on elastic foundations. Balubaid et al. [52] studied free vibration of FG nanoplates using nonlocal two variables integral refined plate theory. Fatima et al. [53] developed a nonlocal zeroth-order shear deformation theory for free vibration of FG nanoscale plates. Hoa et al. [54] developed a nonlocal single variable shear deformation theory to analyze bending and free vibration of FG nanoplates. Zenkour et al. [55-57] analyzed the mechanical and thermal behavior of a carbon nanotube and FG nanoplates via nonlocal shear deformation theory and nonlocal mixed variation formula. Aghababaei [58] developed a combination of nonlocal elasticity theory and third-order shear deformation theory (TSDT) to study static bending and free vibration of nanoplates. Ansari et al. [59] used classical plate theory (CPT), FSDT and higher-order shear deformation theory (HSDT) in combination with nonlocal elasticity theory to analyze buckling of single-layered graphene sheets. Also, molecular dynamics simulations (MDS) have been adopted to analyze and confirm the prediction of the nonlocal plate theories. Hosseini-Hashemi [60] used nonlocal TSDT to study the buckling and free vibration of rectangular nanoplates. The stability and free vibration of FG nanoplates have been studied by Daneshmehr et al. [61,62] via the nonlocal elasticity theory and the HSDT. Malekzadeh et al.

[63] used an extended nonlocal two-variable refined plate theory to analyze the free vibration of nanoplates. A nonlocal two-variable refined plate theory has been developed by Narendar et al. [64,65] to investigate the buckling behavior of orthotropic nanoplates. Sobhy et al. [66-70] developed some nonlocal HSDTs to study the thermal and mechanical behavior of single-layered, double-layered, multi-layered and orthotropic nanoplates. Zenkour et al. [71] examined the thermal buckling of nanoplates lying on Winkler-Pasternak elastic foundations via nonlocal HSDT. A nonlocal sinusoidal plate theory has been developed by Thai et al. [72] to study micro/nanoplates. The thickness stretching effects on the free vibration of nanoplates have been investigated by Bessaim et al. [73] via a nonlocal quasi-3D trigonometric theory. A new quasi-3D theory has been developed by Sobhy et al. [74] to study vibration and buckling of FG nanoplates.

It can be seen that numerous works have been done on the thermal and mechanical behavior analysis of FG nanoplates using differential and integral forms of Eringen's nonlocal elasticity theory. However, most of the available works on free vibration of FG nanoplates using classical Eringen's elasticity theory were carried out with a constant nonlocal parameter, whilst the number of papers on the free vibration analysis of the FG nanoplates with variable nonlocal parameters is still limited (Vinh et al. [75,76], Batra [77]). Therefore, this study focuses on modifying the classical Eringen's nonlocal elasticity theory to consider the variation of the nonlocal parameters through the thickness of the FG nanoplates. The proposed formulations are applied to analyze the free vibration of the power-law and sigmoid FG nanoplates to demonstrate the effects of the variation of the nonlocal parameters on the vibration of the FG nanoplates. Besides, the effects of the side-to-thickness ratio, aspect ratio incorporating with variable nonlocal parameters are investigated carefully.

2. Formulation

2.1. Functionally graded nanoplates

Let's consider a rectangular functionally graded nanoplates with the dimensions of $a \times b$ and the thickness of h. The Cartesian coordinates xyz is located at the middle surface of the FG nanoplates as shown in Figure 1. The distribution of the ceramic and metal components through the thickness of the plate is described via volume fractions with two laws of power-law function and sigmoid function.

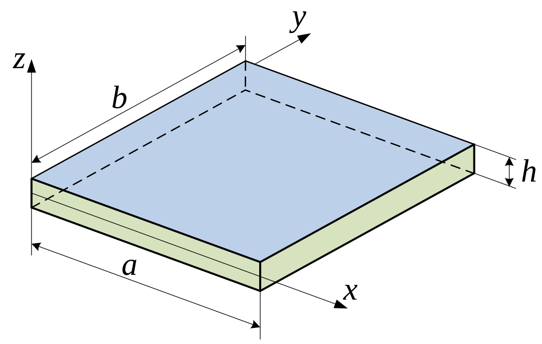

Figure 1. The geometric model of FG nanoplates

2.1.1. Power-law functionally graded nanoplates

In the case of power-law functionally graded (P-FG) nanoplates, the variation of the material properties through the thickness of the plate are computed by

$$X(z) = X_m \left(\frac{X_c}{X_m} \right)^{V_c} \tag{1}$$

where X_c, X_m denote the material properties such as Young's modulus, mass density of the ceramic phase and metal phase, respectively. The volume fraction of the ceramic component, V_c, is obtained as follows

$$V_c = \left(\frac{z}{h} + \frac{1}{2} \right)^k \tag{2}$$

where k is a non-negative power-law index. When $k = 0$, the P-FG nanoplate becomes a full ceramic one, and when $k \to \infty$, the P-FG nanoplate becomes a fully metallic one.

2.1.2. Sigmoid functionally graded nanoplates

The variation of the material properties of the sigmoid functionally graded (S-FG) nanoplates across the thickness direction of the plates are expressed as the following formula

$$X(z) = \begin{cases} \left(1 - V_c^{(1)}\right) X_m + V_c^{(1)} X_c & -h/2 \le z \le 0 \\ V_c^{(2)} X_m + \left(1 - V_c^{(2)}\right) X_c & 0 \le z \le h/2 \end{cases} \tag{3}$$

where $V_c^{(1)}, V_c^{(2)}$ are the volume fractions of ceramic phase, which are calculated by

$$\begin{cases} V_c^{(1)} = \dfrac{1}{2}\left(\dfrac{2z+h}{h}\right)^k & -h/2 \le z \le 0 \\ V_c^{(2)} = \dfrac{1}{2}\left(\dfrac{h-2z}{h}\right)^k & 0 \le z \le h/2 \end{cases} \tag{4}$$

It is obvious that when $k = 0$, the S-FG nanoplate becomes a homogeneous nanoplate of two components (it means the volume fraction of ceramic phase equal to that of metallic phase through the thickness of the plate). When $k \to \infty$, the S-FG nanoplate becomes a two-layer plate with metallic layer at the bottom and ceramic layer at the top of the plate.

2.2. Simple shear deformation theory

2.2.1. Displacement and strain

In this study, a simple shear deformation theory (SSDT) with a new inverse hyperbolic distribution shape function is employed to investigate the free vibration of the FGSW nanoplates. The displacement of the proposed SSDT is written as follows (Narendar [64, 65], Sobhy [66])

$$\begin{aligned} u(x,y,z,t) &= u(x,y,t) - z\frac{\partial w_b}{\partial x} + f(z)\frac{\partial w_s}{\partial x} \\ v(x,y,z,t) &= v(x,y,t) - z\frac{\partial w_b}{\partial y} + f(z)\frac{\partial w_s}{\partial y} \\ w(x,y,z,t) &= w_b(x,y,t) + w_s(x,y,t) \end{aligned} \tag{5}$$

where $f(z)$ is the inverse hyperbolic distribution shape function, which is given by

$$f(z) = \left(\frac{5}{4}\pi h - 5\pi^3 h\right)\tanh^{-1}\left(\frac{z}{\pi h}\right) + \left(5\pi^2 - 1\right)z \tag{6}$$

The new inverse hyperbolic distribution shape function $f(z)$ satisfies free conditions of the transverse shear stress on two surfaces of the plates and the nonlinear distribution through the thickness of the plates. So, the proposed SSDT does not need any shear correction factor. The strains fields of the plate are obtained as

$$
\begin{aligned}
\varepsilon_x &= \frac{\partial u}{\partial x} - z\frac{\partial^2 w_b}{\partial x^2} + f\,\frac{\partial^2 w_s}{\partial x^2} \\
\varepsilon_y &= \frac{\partial v}{\partial y} - z\frac{\partial^2 w_b}{\partial y^2} + f\,\frac{\partial^2 w_s}{\partial y^2} \\
\gamma_{xy} &= \frac{\partial u}{\partial y} + \frac{\partial v}{\partial x} - 2z\frac{\partial^2 w_b}{\partial x \partial y} + 2f\,\frac{\partial^2 w_s}{\partial x \partial y} \\
\gamma_{xz} &= g\,\frac{\partial w_s}{\partial x} \\
\gamma_{yz} &= g\,\frac{\partial w_s}{\partial x}
\end{aligned}
\tag{7}
$$

where $g(z) = 1 + f'(z)$. In the matrix form

$$
\begin{Bmatrix} \varepsilon_x \\ \varepsilon_y \\ \gamma_{xy} \end{Bmatrix} = \begin{Bmatrix} \varepsilon_x^m \\ \varepsilon_y^m \\ \gamma_{xy}^m \end{Bmatrix} + z\begin{Bmatrix} \varepsilon_x^b \\ \varepsilon_y^b \\ \gamma_{xy}^b \end{Bmatrix} + f(z)\begin{Bmatrix} \varepsilon_x^s \\ \varepsilon_y^s \\ \gamma_{xy}^s \end{Bmatrix}, \begin{Bmatrix} \gamma_{xz} \\ \gamma_{yz} \end{Bmatrix} = g(z)\begin{Bmatrix} \gamma_{xz}^0 \\ \gamma_{yz}^0 \end{Bmatrix}
\tag{8}
$$

In which

$$
\begin{Bmatrix} \varepsilon_x^m \\ \varepsilon_y^m \\ \gamma_{xy}^m \end{Bmatrix} = \begin{Bmatrix} \dfrac{\partial u}{\partial x} \\ \dfrac{\partial v}{\partial y} \\ \dfrac{\partial u}{\partial y} + \dfrac{\partial v}{\partial x} \end{Bmatrix}, \begin{Bmatrix} \varepsilon_x^b \\ \varepsilon_y^b \\ \gamma_{xy}^b \end{Bmatrix} = -\begin{Bmatrix} \dfrac{\partial^2 w_b}{\partial x^2} \\ \dfrac{\partial^2 w_b}{\partial y^2} \\ 2\dfrac{\partial^2 w_b}{\partial x \partial y} \end{Bmatrix}, \begin{Bmatrix} \varepsilon_x^s \\ \varepsilon_y^s \\ \gamma_{xy}^s \end{Bmatrix} = \begin{Bmatrix} \dfrac{\partial^2 w_s}{\partial x^2} \\ \dfrac{\partial^2 w_s}{\partial y^2} \\ 2\dfrac{\partial^2 w_s}{\partial x \partial y} \end{Bmatrix}, \begin{Bmatrix} \gamma_{xz}^0 \\ \gamma_{yz}^0 \end{Bmatrix} = \begin{Bmatrix} \dfrac{\partial w_s}{\partial x} \\ \dfrac{\partial w_s}{\partial y} \end{Bmatrix}
\tag{9}
$$

2.2.2. Constitutive relations

The constitutive equations of the plate are expressed as (Thai et al. [72])

$$
\begin{Bmatrix} \sigma_x \\ \sigma_y \\ \tau_{xy} \end{Bmatrix} = \begin{bmatrix} \Theta_{11} & \Theta_{12} & 0 \\ \Theta_{12} & \Theta_{22} & 0 \\ 0 & 0 & \Theta_{66} \end{bmatrix} \begin{Bmatrix} \varepsilon_x \\ \varepsilon_y \\ \gamma_{xy} \end{Bmatrix}
\tag{10}
$$

$$
\begin{Bmatrix} \tau_{yz} \\ \tau_{xz} \end{Bmatrix} = \begin{bmatrix} \Theta_{44} & 0 \\ 0 & \Theta_{55} \end{bmatrix} \begin{Bmatrix} \gamma_{yz} \\ \gamma_{xz} \end{Bmatrix}
\tag{11}
$$

where

$$\Theta_{11}=\Theta_{22}=\frac{E(z)}{1-\nu(z)^2},\ \Theta_{44}=\Theta_{55}=\Theta_{66}=\frac{E(z)}{2\left(1+\nu(z)\right)},\Theta_{12}=\nu(z)\Theta_{11} \tag{12}$$

2.3. The nonlocal elasticity theory

Eringen [1-3] developed a nonlocal elasticity theory to study nanoscale structures with integral and differential form. The differential form of the classical nonlocal elasticity theory of Eringen is as the following formula (Eringen [1-3])

$$\left(1-\mu\nabla^2\right)\sigma_{ij}=t_{ij} \tag{13}$$

where σ_{ij}, t_{ij} are respectively the nonlocal and local stress tensors, $\nabla^2=\partial^2/\partial x^2+\partial^2/\partial y^2$ is the second Laplace operator, $\mu=\left(e_0 a\right)^2$ (nm^2) is the nonlocal parameter, in which e_0 is a material constant which is determined via experimental or simulation of atomistic dynamic, a is an internal characteristic length which depends on the distance of the molecules, diameter of lattice, and granular size. It is obvious that these coefficients are the material-dependent parameters. It is noticed that the differential form of the classical Eringen's nonlocal elasticity theory is developed based on the assumption of the constant nonlocal parameter. So, the classical nonlocal elasticity theory in the differential form is only suitable for the analysis of isotropic and homogeneous structures. In the cases of FG plates, the material properties, including nonlocal parameter, vary through the thickness of the plates as well. So, the variation of the nonlocal parameter must be considered (). By making a further assumption of the variation of the nonlocal parameter through the thickness direction of the FG plates, the nonlocal constitutive relations of the nanoplates can be expressed as follows

$$\begin{Bmatrix} t_x \\ t_y \\ t_{xy} \end{Bmatrix}=\left(1-\mu(z)\nabla^2\right)\begin{Bmatrix} \sigma_x \\ \sigma_y \\ \tau_{xy} \end{Bmatrix}=\begin{bmatrix} \Theta_{11} & \Theta_{12} & 0 \\ \Theta_{12} & \Theta_{22} & 0 \\ 0 & 0 & \Theta_{66} \end{bmatrix}\begin{Bmatrix} \varepsilon_x \\ \varepsilon_y \\ \gamma_{xy} \end{Bmatrix} \tag{14}$$

$$\begin{Bmatrix} t_{yz} \\ t_{xz} \end{Bmatrix}=\left(1-\mu(z)\nabla^2\right)\begin{Bmatrix} \tau_{yz} \\ \tau_{xz} \end{Bmatrix}=\begin{bmatrix} \Theta_{44} & 0 \\ 0 & \Theta_{55} \end{bmatrix}\begin{Bmatrix} \gamma_{yz} \\ \gamma_{xz} \end{Bmatrix} \tag{15}$$

Therefore, the ratio between the nonlocal parameter of the ceramic phase and the metal phase $\lambda = \mu_c / \mu_m$ is introduced as a new parameter. It is obvious that the classical Eringen's nonlocal elasticity theory can be obtained by setting $\mu(z) = \mu_m = \mu_c = \text{const}$ or $\lambda = \mu_c / \mu_m = 1$. According to the present nonlocal constitutive relations, it can be seen that the small-scale effects not only vary through the in-plane directions but also vary through the thickness direction of the nanoplates. Hence, the present nonlocal elasticity theory is completely different from the classical nonlocal elasticity theory where the small-scale effects are similar through the thickness direction of the nanoplates. The proposed formulations can be applied in a wide range of engineering computations for micro/nanostructures.

2.4. Equations of motion

The variation form of Hamilton's principle is employed to obtain the governing equations of motion as the following formula

$$0 = \int_0^T \left(\delta U - \delta K \right) dt \tag{16}$$

where δU is the variation of the strain energy and δK is the variation of the kinematic energy of the plate. The expression of the variation of the strain energy is calculated as follows (Thai et al. [72])

$$\delta U = \int_A \int_{-h/2}^{h/2} \left(\sigma_x \delta \varepsilon_x + \sigma_y \delta \varepsilon_y + \tau_{xy} \delta \varepsilon_{xy} + \tau_{xz} \delta \varepsilon_{xz} + \tau_{yz} \delta \varepsilon_{yz} \right) dz dA \tag{17}$$

The variation of the kinetic energy of the plate is calculated as follows (Thai et al. [72])

$$\delta K = \int_A \int_{-h/2}^{h/2} \left(\dot{u} \delta \dot{u} + \dot{v} \delta \dot{v} + \dot{w} \delta \dot{w} \right) \rho(z) dz dA \tag{18}$$

By introducing Eqs. (7), (10), and (11) into Eq. (17), substituting Eq. (5) into Eq. (18) and considering the nonlocal relations of Eqs. (14) and (15), the governing equations of motion of the nanoplates are derived from Eq. (16) as the following formulae

$$
\begin{aligned}
&\delta u:\frac{\partial N_x}{\partial x}+\frac{\partial N_{xy}}{\partial y}=I_0\ddot{u}-I_1\frac{\partial \ddot{w}_b}{\partial x}+I_2\frac{\partial \ddot{w}_s}{\partial x}-\nabla^2\left(J_0\ddot{u}-J_1\frac{\partial \ddot{w}_b}{\partial x}+J_2\frac{\partial \ddot{w}_s}{\partial x}\right)\\
&\delta v:\frac{\partial N_y}{\partial y}+\frac{\partial N_{xy}}{\partial x}=I_0\ddot{v}-I_1\frac{\partial \ddot{w}_b}{\partial y}+I_2\frac{\partial \ddot{w}_s}{\partial y}-\nabla^2\left(J_0\ddot{u}-J_1\frac{\partial \ddot{w}_b}{\partial x}+J_2\frac{\partial \ddot{w}_s}{\partial x}\right)\\
&\delta w_b:\frac{\partial^2 M_x}{\partial x^2}+2\frac{\partial^2 M_{xy}}{\partial x\partial y}+\frac{\partial^2 M_y}{\partial y^2}=I_0(\ddot{w}_b+\ddot{w}_s)+I_1\left(\frac{\partial \ddot{u}}{\partial x}+\frac{\partial \ddot{v}}{\partial y}\right)-\nabla^2\left(I_3\ddot{w}_b-I_4\ddot{w}_s\right)\\
&\qquad\qquad -\nabla^2\left[J_0(\ddot{w}_b+\ddot{w}_s)+J_1\left(\frac{\partial \ddot{u}}{\partial x}+\frac{\partial \ddot{v}}{\partial y}\right)-\nabla^2\left(J_3\ddot{w}_b-J_4\ddot{w}_s\right)\right]\\
&\delta w_s:\frac{\partial^2 L_x}{\partial x^2}+2\frac{\partial^2 L_{xy}}{\partial x\partial y}+\frac{\partial^2 L_y}{\partial y^2}-\frac{\partial R_x}{\partial x}-\frac{\partial R_y}{\partial y}=-I_0(\ddot{w}_b+\ddot{w}_s)+I_2\left(\frac{\partial \ddot{u}}{\partial x}+\frac{\partial \ddot{v}}{\partial y}\right)-\nabla^2\left(I_4\ddot{w}_b-I_5\ddot{w}_s\right)\\
&\qquad\qquad -\nabla^2\left[-J_0(\ddot{w}_b+\ddot{w}_s)+J_2\left(\frac{\partial \ddot{u}}{\partial x}+\frac{\partial \ddot{v}}{\partial y}\right)-\nabla^2\left(J_4\ddot{w}_b-J_5\ddot{w}_s\right)\right]
\end{aligned}
\tag{19}
$$

where N_i, M_i, L_i and R_i are the local stress resultants which are calculated by

$$
\begin{aligned}
&\begin{Bmatrix} N_x \\ N_y \\ N_{xy} \end{Bmatrix}=\int_{-h/2}^{h/2}\begin{Bmatrix} t_x \\ t_y \\ t_{xy} \end{Bmatrix}dz,\qquad \begin{Bmatrix} M_x \\ M_y \\ M_{xy} \end{Bmatrix}=\int_{-h/2}^{h/2}\begin{Bmatrix} t_x \\ t_y \\ t_{xy} \end{Bmatrix}zdz\\
&\begin{Bmatrix} L_x \\ L_y \\ L_{xy} \end{Bmatrix}=\int_{-h/2}^{h/2}\begin{Bmatrix} t_x \\ t_y \\ t_{xy} \end{Bmatrix}f(z)dz,\quad \begin{Bmatrix} R_x \\ R_y \end{Bmatrix}=\int_{-h/2}^{h/2}\begin{Bmatrix} t_{xz} \\ t_{yz} \end{Bmatrix}g(z)dz
\end{aligned}
\tag{20}
$$

By substituting Eqs. (14) and (15) into Eq. (20) and integrating through the thickness of the nanoplates, then reordering these equations into matrix form, one gets

$$
\begin{Bmatrix} N_x \\ N_y \\ N_{xy} \end{Bmatrix}=\begin{bmatrix} A_{11} & A_{12} & 0 \\ A_{12} & A_{22} & 0 \\ 0 & 0 & A_{66} \end{bmatrix}\begin{Bmatrix} \varepsilon_x^m \\ \varepsilon_y^m \\ \gamma_{xy}^m \end{Bmatrix}+\begin{bmatrix} B_{11} & B_{12} & 0 \\ B_{12} & B_{22} & 0 \\ 0 & 0 & B_{66} \end{bmatrix}\begin{Bmatrix} \varepsilon_x^b \\ \varepsilon_y^b \\ \gamma_{xy}^b \end{Bmatrix}+\begin{bmatrix} E_{11} & E_{12} & 0 \\ E_{12} & E_{22} & 0 \\ 0 & 0 & E_{66} \end{bmatrix}\begin{Bmatrix} \varepsilon_x^s \\ \varepsilon_y^s \\ \gamma_{xy}^s \end{Bmatrix}
\tag{21}
$$

$$
\begin{Bmatrix} M_x \\ M_y \\ M_{xy} \end{Bmatrix}=\begin{bmatrix} B_{11} & B_{12} & 0 \\ B_{12} & B_{22} & 0 \\ 0 & 0 & B_{66} \end{bmatrix}\begin{Bmatrix} \varepsilon_x^m \\ \varepsilon_y^m \\ \gamma_{xy}^m \end{Bmatrix}+\begin{bmatrix} D_{11} & D_{12} & 0 \\ D_{12} & D_{22} & 0 \\ 0 & 0 & D_{66} \end{bmatrix}\begin{Bmatrix} \varepsilon_x^b \\ \varepsilon_y^b \\ \gamma_{xy}^b \end{Bmatrix}+\begin{bmatrix} F_{11} & F_{12} & 0 \\ F_{12} & F_{22} & 0 \\ 0 & 0 & F_{66} \end{bmatrix}\begin{Bmatrix} \varepsilon_x^s \\ \varepsilon_y^s \\ \gamma_{xy}^s \end{Bmatrix}
\tag{22}
$$

$$
\begin{Bmatrix} L_x \\ L_y \\ L_{xy} \end{Bmatrix}=\begin{bmatrix} E_{11} & E_{12} & 0 \\ E_{12} & E_{22} & 0 \\ 0 & 0 & E_{66} \end{bmatrix}\begin{Bmatrix} \varepsilon_x^m \\ \varepsilon_y^m \\ \gamma_{xy}^m \end{Bmatrix}+\begin{bmatrix} F_{11} & F_{12} & 0 \\ F_{12} & F_{22} & 0 \\ 0 & 0 & F_{66} \end{bmatrix}\begin{Bmatrix} \varepsilon_x^b \\ \varepsilon_y^b \\ \gamma_{xy}^b \end{Bmatrix}+\begin{bmatrix} H_{11} & H_{12} & 0 \\ H_{12} & H_{22} & 0 \\ 0 & 0 & H_{66} \end{bmatrix}\begin{Bmatrix} \varepsilon_x^s \\ \varepsilon_y^s \\ \gamma_{xy}^s \end{Bmatrix}
\tag{23}
$$

$$\begin{Bmatrix} R_x \\ R_y \end{Bmatrix} = \begin{bmatrix} S_{44} & 0 \\ 0 & S_{55} \end{bmatrix} \begin{Bmatrix} \gamma_{xz}^0 \\ \gamma_{yz}^0 \end{Bmatrix} \tag{24}$$

where

$$\left(A_{ij}, B_{ij}, E_{ij}, D_{ij}, F_{ij}, H_{ij}\right) = \int_{-h/2}^{h/2} \Theta_{ij} \left(1, z, f(z), z^2, zf(z), f^2(z)\right) dz \tag{25}$$

$$\left(S_{ij}\right) = \int_{-h/2}^{h/2} \Theta_{ij} \left(g^2(z)\right) dz \tag{26}$$

In the case of the conventional nonlocal elasticity theory, the nonlocal parameter μ is assumed to be constant through the thickness of the nanoplates. So, the coefficients $I_0, I_1, I_2, I_3, I_4, I_5$ and $J_0, J_1, J_2, J_3, J_4, J_5$ are calculated as the following formulae

$$\left(I_0, I_1, I_2, I_3, I_4, I_5\right) = \int_{-h/2}^{h/2} \rho(z) \left(1, z, f(z), z^2, zf(z), f^2(z)\right) dz \tag{27}$$

$$\left(J_0, J_1, J_2, J_3, J_4, J_5\right) = \mu \int_{-h/2}^{h/2} \rho(z) \left(1, z, f(z), z^2, zf(z), f^2(z)\right) dz \tag{28}$$

It is obvious that when the nonlocal parameter μ is constant, one gets $J_i = \mu I_i$. Consequently, the governing equations of motion Eq. (19) become the conventional governing equations of motion of the nanoplates with a constant nonlocal parameter, which is usually used by many researchers in the literature. In this study, the nonlocal parameter is assumed to vary through the thickness of the nanoplates as other material properties. Thus, the coefficients $I_0, I_1, I_2, I_3, I_4, I_5$ are calculated via Eq. (27), while the coefficients $J_0, J_1, J_2, J_3, J_4, J_5$ are calculated as follows

$$\left(J_0, J_1, J_2, J_3, J_4, J_5\right) = \int_{-h/2}^{h/2} \mu(z) \rho(z) \left(1, z, f(z), z^2, zf(z), f^2(z)\right) dz \tag{29}$$

2.5. Navier's solution

In this study, an FG nanoplate subjected to simply supported at all edges is considered. The Navier's solution technique is employed to solve the equations of motion, the unknown displacement functions of the nanoplates are assumed as the following formulae (Narendar [64, 65])

$$
\begin{aligned}
u(x,y,t) &= \sum_{m=1}^{\infty}\sum_{n=1}^{\infty} U_{mn}\, e^{i\omega t}\cos\alpha x \sin\beta y \\
v(x,y,t) &= \sum_{m=1}^{\infty}\sum_{n=1}^{\infty} V_{mn}\, e^{i\omega t}\sin\alpha x \cos\beta y \\
w_b(x,y,t) &= \sum_{m=1}^{\infty}\sum_{n=1}^{\infty} Wb_{mn}\, e^{i\omega t}\sin\alpha x \sin\beta y \\
w_s(x,y,t) &= \sum_{m=1}^{\infty}\sum_{n=1}^{\infty} Ws_{mn}\, e^{i\omega t}\sin\alpha x \sin\beta y
\end{aligned}
\tag{30}
$$

where $\alpha = m\pi / a$ and $\beta = n\pi / b$, $\left(U_{mn}, V_{mn}, Wb_{mn}, Ws_{mn}\right)$ are the unknown coefficients, ω is the frequency of the FG nanoplates.

Substituting Eq. (30) into Eq. (7) and then Eq. (19), one gets

$$
\left(\mathbf{K} - \omega^2 \mathbf{M}\right)\begin{Bmatrix} U_{mn} \\ V_{mn} \\ Wb_{mn} \\ Ws_{mn} \end{Bmatrix} = \mathbf{0}
\tag{31}
$$

where $\mathbf{K}, \mathbf{M}$ are the stiffness matrix and mass matrix, and those element are $K_{ij}, M_{ij}, i, j = \overline{1,4}$ which are calculated as the following formulae

$$
\begin{aligned}
&K_{11} = A_{11}\alpha^2 + A_{66}\beta^2; K_{12} = \beta\left(A_{12} + A_{66}\right)\alpha; \\
&K_{13} = -B_{11}\alpha^3 + \left(-B_{12} - 2B_{66}\right)\beta^2\alpha; K_{14} = E_{11}\alpha^3 + \left(E_{12} + 2E_{66}\right)\beta^2\alpha; \\
&K_{22} = A_{22}\beta^2 + A_{66}\alpha^2; K_{23} = -B_{22}\beta^3 - \left(B_{12} + 2B_{66}\right)\alpha^2\beta; \\
&K_{24} = E_{22}\beta^3 + \left(E_{12} + 2E_{33}\right)\alpha^2\beta; K_{33} = D_{11}\alpha^4 + 2\left(D_{12} + 2D_{66}\right)\beta^2\alpha^2 + D_{22}\beta^4; \\
&K_{34} = -F_{11}\alpha^4 - 2\left(F_{12} + 2F_{66}\right)\beta^2\alpha^2 - F_{22}\beta^4; \\
&K_{44} = H_{11}\alpha^4 + \left(\left(2H_{12} + 4H_{66}\right)\beta^2 + As_{55}\right)\alpha^2 + \left(H_{22}\beta^2 + As_{44}\right)\beta^2.
\end{aligned}
\tag{32}
$$

$$\begin{aligned}
&M_{11}=\left(\alpha^2+\beta^2\right)J_0+I_0; M_{12}=0; M_{13}=-\left(\left(\alpha^2+\beta^2\right)J_1+I_1\right)\alpha;\\
&M_{14}=\left(\left(\alpha^2+\beta^2\right)J_2+I_2\right)\alpha; M_{22}=\left(\alpha^2+\beta^2\right)J_0+I_0;\\
&M_{23}=-\left(\left(\alpha^2+\beta^2\right)J_1+I_1\right)\beta; M_{24}=\left(\left(\alpha^2+\beta^2\right)J_2+I_2\right)\beta;\\
&M_{33}=J_3\alpha^4+\left(2J_3\beta^2+I_3+J_0\right)\alpha^2+J_3\beta^4+\left(I_3+J_0\right)\beta^2+I_0;\\
&M_{34}=-J_4\alpha^4+\left(-2J_4\beta^2-I_4+J_0\right)\alpha^2-J_4\beta^4+\left(-I_4+J_0\right)\beta^2+I_0;\\
&M_{44}=J_5\alpha^4+\left(2J_5\beta^2+I_5+J_0\right)\alpha^2+J_5\beta^4+\left(I_5+J_0\right)\beta^2+I_0.
\end{aligned} \tag{33}$$

By solving Eq. (31), the frequencies and responding eigenvectors of the nanoplates are achieved.

3. Numerical results

3.1. Verification study

Firstly, the numerical results of free vibration of FG nanoplates using the proposed theory are compared with those of Sobhy et al. [74]. In this subsection, the FG nanoplates are made of $Si_3N_4/SUS304$ with several values of side-to-thickness ratios a/h and nonlocal parameters μ are considered. The dimensions of the plates are $a=b=10$ nm, the material properties of Si_3N_4 are $E_c=348.43$ GPa, $\rho_c=2370$ kg/m^3, $\nu_c=0.24$, whereas those of SUS304 are $E_m=201.04$ GPa, $\rho_m=8166$ kg/m^3, $\nu_m=0.3$. The effective material properties are calculated via the power-law function by $X(z)=X_m+\left(X_c-X_m\right)\left(z/h+0.5\right)^k$. The comparison between the non-dimensional fundamental frequencies $\bar{\omega}=10\omega h\sqrt{\rho_m/E_m}$ of the FG nanoplates of $Si_3N_4/SUS304$ using present theory and those of Sobhy et al. [74] using higher-order shear deformation theory (HSDT) and quasi-3D theory are shown in Table 1. According to this table, it can be concluded that the present results are in good agreement with those of Sobhy et al. [74].

Table 1. The comparison of the non-dimensional fundamental frequencies of the FG nanoplates of $Si_3N_4/SUS304$ with power-law scheme

a/h	k	Theory	$\mu=0^2$	$\mu=0.5^2$	$\mu=1^2$	$\mu=1.5^2$	$\mu=2^2$
5	0	Sobhy et al. [74] (HSDT)	5.10702	4.98549	4.66713	4.24976	3.81763
		Sobhy et al. [74] (quasi-3D)	5.12377	5.00184	4.68243	4.26370	3.83015

		Present	5.10680	4.98527	4.66692	4.24957	3.81746
	1	Sobhy et al. [74] (HSDT)	3.01860	2.94677	2.75859	2.51190	2.25648
		Sobhy et al. [74] (quasi-3D)	3.04445	2.97200	2.78221	2.53340	2.27580
		Present	3.01894	2.94709	2.75890	2.51218	2.25673
	5	Sobhy et al. [74] (HSDT)	2.42443	2.36674	2.21560	2.01747	1.81232
		Sobhy et al. [74] (quasi-3D)	2.44172	2.38362	2.23140	2.03185	1.82525
		Present	2.42459	2.36690	2.21575	2.01760	1.81244
	Metal	Sobhy et al. [74] (HSDT)	2.11261	2.06234	1.93064	1.75799	1.57923
		Sobhy et al. [74] (quasi-3D)	2.12231	2.07180	1.93950	1.76606	1.58648
		Present	2.11252	2.06225	1.93056	1.75792	1.57916
10	0	Sobhy et al. [74] (HSDT)	1.38829	1.35525	1.26871	1.15525	1.03778
		Sobhy et al. [74] (quasi-3D)	1.39015	1.35707	1.27041	1.15680	1.03917
		Present	1.38826	1.35523	1.26869	1.15523	1.03776
	1	Sobhy et al. [74] (HSDT)	0.82250	0.80292	0.75165	0.68443	0.61484
		Sobhy et al. [74] (quasi-3D)	0.82782	0.80812	0.75652	0.68886	0.61882
		Present	0.82294	0.80336	0.75206	0.68481	0.61517
	5	Sobhy et al. [74] (HSDT)	0.66485	0.64903	0.60758	0.55325	0.49699
		Sobhy et al. [74] (quasi-3D)	0.66890	0.65299	0.61129	0.55662	0.50002
		Present	0.66512	0.64929	0.60783	0.55347	0.49719
	Metal	Sobhy et al. [74] (HSDT)	0.57695	0.56322	0.52725	0.48010	0.43128
		Sobhy et al. [74] (quasi-3D)	0.57817	0.56441	0.52837	0.48112	0.43220
		Present	0.57694	0.56321	0.52725	0.48010	0.43128
20	0	Sobhy et al. [74] (HSDT)	0.35558	0.34712	0.32495	0.29589	0.26581
		Sobhy et al. [74] (quasi-3D)	0.35584	0.34737	0.32519	0.29611	0.26600
		Present	0.35558	0.34712	0.32495	0.29589	0.26581
	1	Sobhy et al. [74] (HSDT)	0.21083	0.20581	0.19267	0.17544	0.15760
		Sobhy et al. [74] (quasi-3D)	0.21205	0.20701	0.19379	0.17646	0.15851
		Present	0.21098	0.20596	0.19280	0.17556	0.15771
	5	Sobhy et al. [74] (HSDT)	0.17077	0.16671	0.15606	0.14210	0.12765
		Sobhy et al. [74] (quasi-3D)	0.17175	0.16767	0.15696	0.14292	0.12839
		Present	0.17086	0.16680	0.15614	0.14218	0.12772
	Metal	Sobhy et al. [74] (HSDT)	0.14799	0.14447	0.13524	0.12315	0.11063
		Sobhy et al. [74] (quasi-3D)	0.14819	0.14466	0.13543	0.12331	0.11078
		Present	0.14800	0.14448	0.13525	0.12315	0.11063

Continuously, the non-dimensional frequencies of the square FG nanoplates with the material properties are calculated via the Mori-Tanaka homogenization scheme are examined. The present numerical results using the proposed algorithm are compared with those of Fatima et al. [53] using nonlocal zeroth-order deformation theory. The FG nanoplates are made of Si_3N_4/SUS304 with the material properties of each individual component are similar to those in the previous comparison, but the Poisson's ratio of both components are assumed to be constant $\nu_m = \nu_m = \nu = 0.3$. The dimensions of the nanoplates are $a = b = 10$ nm, the effective Young's modulus and Poisson's ratio of the nanoplates are calculated via Mori-Tanaka homogenization scheme while the effective mass density is calculated via mixtures scheme as follows (Fatima et al. [53])

$$E = \frac{9KG}{3K+G}, \nu = \frac{3K-2G}{2(3K+G)} \tag{34}$$

$$\rho = \rho_c V_c + \rho_m (1 - V_c) \tag{35}$$

where

$$\begin{aligned} \frac{K-K_m}{K_c-K_m} &= \frac{V_c}{1+(1-V_c)\dfrac{3(K_c-K_m)}{3K_m+4G_m}} \\ \frac{G-G_m}{G_c-G_m} &= \frac{V_c}{1+(1-V_c)\dfrac{(G_c-G_m)}{G_m+G_f}} \end{aligned} \tag{36}$$

with

$$G_f = \frac{G_m(9K_m+8G_m)}{6(K_m+2G_m)}, \; V_c = \left(\frac{z+h/2}{h}\right)^k \tag{37}$$

The non-dimensional frequency is calculated as

$$\hat{\omega} = \omega h \sqrt{\frac{\rho_m}{E_m}} \tag{38}$$

The non-dimensional fundamental frequencies of the FG nanoplates using present theory and those of Fatima et al. [53] are presented in Table 2. The comparison shows that the present numerical results are closed to the solutions of Fatima et al. [53].

According to the two above comparison studies. It can be concluded that the present algorithm is suitable for the examination of the FG nanoplates.

Table 2. The comparison of the non-dimensional fundamental frequencies of the FG nanoplates of $Si_3N_4/SUS304$ with Mori-Tanaka scheme

a/h	μ	$k=0$		$k=1$		$k=5$	
		Fatima et al. [53]	Present	Fatima et al. [53]	Present	Fatima et al. [53]	Present
10	0	0.1409	0.14099	0.0793	0.08216	0.0655	0.06637
	1	0.1288	0.12884	0.0725	0.07509	0.0599	0.06066
	2	0.1193	0.11938	0.0672	0.06957	0.0555	0.05620
	3	0.1117	0.11173	0.0629	0.06512	0.0519	0.05260
	4	0.1053	0.10539	0.0593	0.06142	0.0490	0.04962
20	0	0.0361	0.03617	0.0203	0.02109	0.0168	0.01705
	1	0.0330	0.03305	0.0186	0.01927	0.0153	0.01559
	2	0.0306	0.03062	0.0172	0.01786	0.0142	0.01444
	3	0.0286	0.02866	0.0161	0.01671	0.0133	0.01352
	4	0.0270	0.02703	0.0152	0.01576	0.0125	0.01275

3.2. Parameter study

In this section, a functionally graded nanoplates of Al/ZrO_2 with a constant area of $S = a.b = 100\,(\text{nm}^2)$ is considered. The material properties of Al are $E_m = 70\,\text{GPa}$, $\rho_m = 2707\,\text{kg/m}^3$, $\nu_m = 0.3$ and those of ZrO_2 are $E_c = 151\,\text{GPa}$, $\rho_c = 3000\,\text{kg/m}^3$, $\nu_c = 0.3$. The nonlocal parameter of the metal phase of Al is constant and taken as $\mu_m = 2\,(\text{nm}^2)$, and it plays as reference nonlocal value. The variation of the effective Young's modulus, mass density and nonlocal parameter through the thickness of the P-FG and S-FG nanoplates are presented in Figures 2-4. For convenience, the non-dimensional frequencies are calculated as

$$\omega^* = \omega \frac{S}{h_0}\sqrt{\frac{\rho_0}{E_0}},\ h_0 = \frac{\sqrt{S}}{10},\ \rho_0 = 1\,\text{kg/m}^3,\ E_0 = 1\,\text{GPa} \tag{39}$$

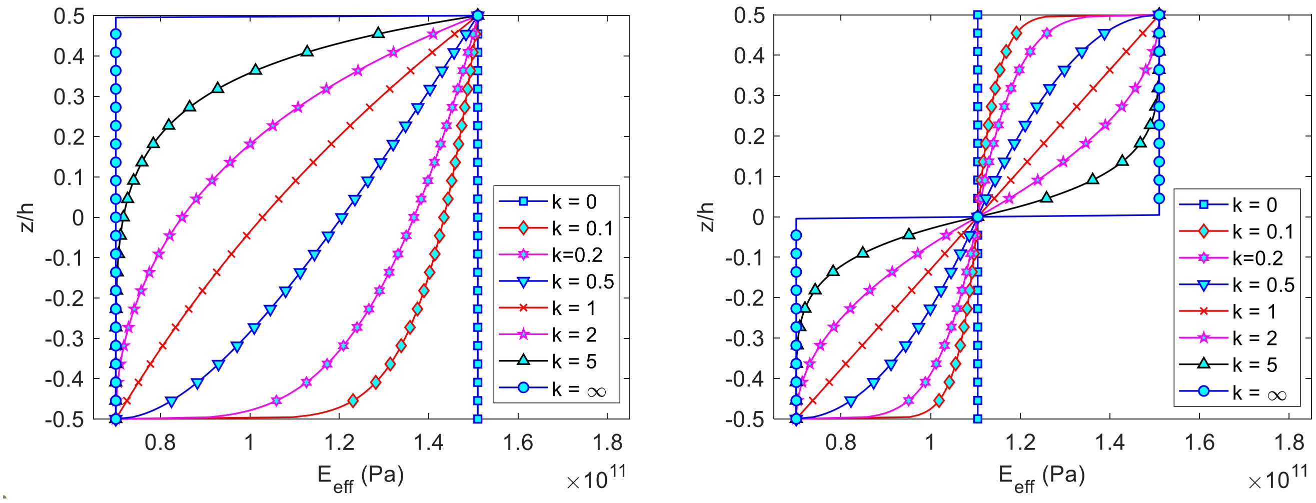

a) P-FG

b) S-FG

Figure 2. The variation of the effective Young's modulus through the thickness of the FG nanoplates

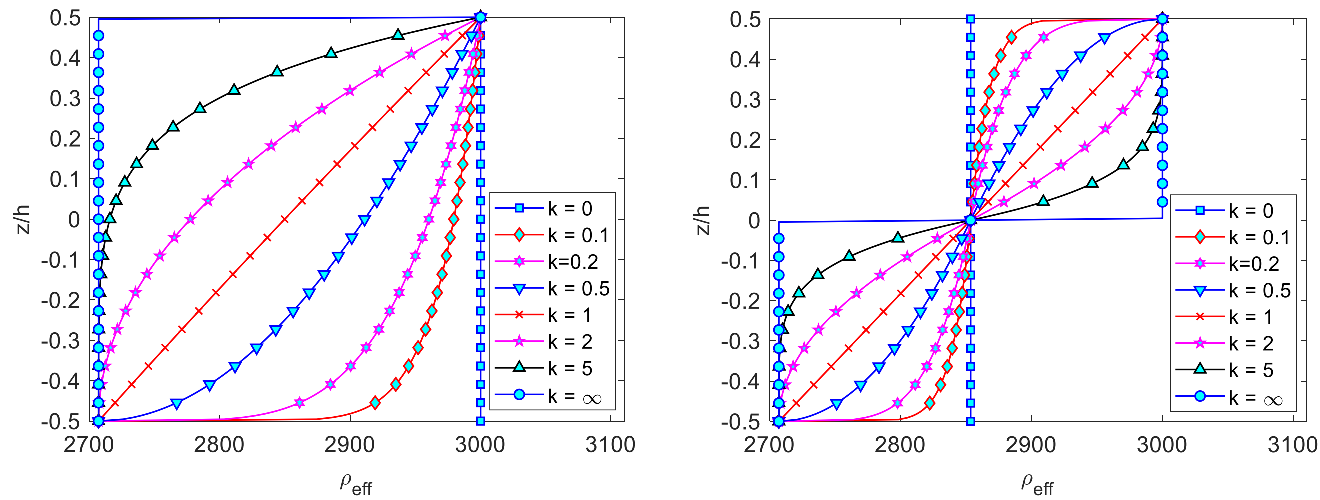

a) P-FG

b) S-FG

Figure 3. The variation of the effective mass density through the thickness of the FG nanoplates

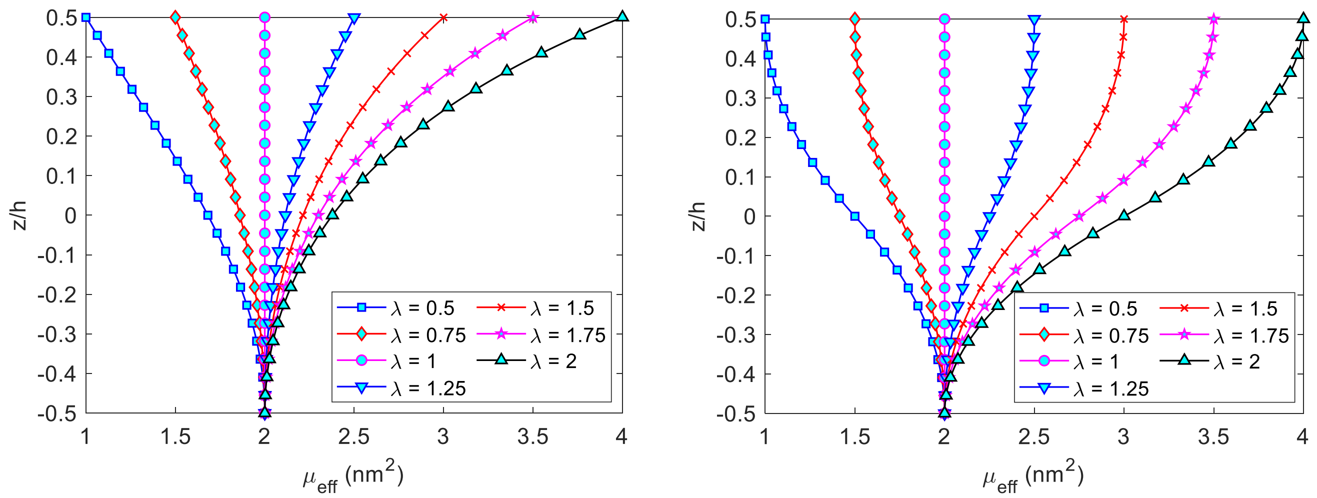

a) P-FG b) S-FG

Figure 4. The variation of the effective nonlocal parameter through the thickness of the FG nanoplates ($k = 2$)

Firstly, the non-dimensional fundamental frequencies of the square P-FG and S-FG nanoplates with several values of material parameter k and ratio of nonlocal parameters are given in Table 3. The dimensions of the nanoplates are $a = b = 10\ (\mathrm{nm}^2)$, the thickness of the nanoplates is $h = a/10$. From Table 3, it can see clearly that when the ratio of the nonlocal parameters increases, the fundamental frequencies of the nanoplates decrease. In general, when the power-law index k increases, the fundamental frequencies of the P-FG and S-FG nanoplates decreases. However, the frequency of the P-FG nanoplates decrease faster than those of the S-FG nanoplates. The reason is that when the power-law index increases, the volume fraction of ceramic of the P-FG nanoplates increases, so the stiffness of the P-FG nanoplates increase rapidly. In the case of S-FG nanoplates, both volume fractions of ceramic and metal increase when the power-law index increases, so the stiffness of the S-FG nanoplates increase slower than that of the P-FG nanoplates.

Table 3. The non-dimensional fundamental frequency of the square P-FG and S-FG nanoplates

Types	λ	$k=0$	$k=0.25$	$k=0.5$	$k=1$	$k=2$	$k=5$	$k=10$
P-FG	0.5	1.18288	1.07773	1.02145	0.96498	0.92212	0.88136	0.85256
	0.75	1.13695	1.04194	0.99222	0.94357	0.90810	0.87446	0.84886
	1	1.09599	1.01125	0.96754	0.92569	0.89643	0.86871	0.84577
	1.25	1.05916	0.98423	0.94596	0.91010	0.88624	0.86367	0.84305
	1.5	1.02581	0.96003	0.92669	0.89616	0.87710	0.85912	0.84059

	1.75	0.99542	0.93810	0.90921	0.88350	0.86875	0.85494	0.83832
	2	0.96758	0.91804	0.89321	0.87185	0.86104	0.85105	0.83620
S-FG	0.5	0.99726	0.99332	0.98695	0.97608	0.96399	0.95369	0.95070
	0.75	0.97880	0.97488	0.96854	0.95776	0.94574	0.93545	0.93243
	1	0.96133	0.95743	0.95114	0.94042	0.92848	0.91822	0.91517
	1.25	0.94476	0.94089	0.93463	0.92400	0.91214	0.90191	0.89884
	1.5	0.92902	0.92517	0.91896	0.90841	0.89663	0.88644	0.88335
	1.75	0.91404	0.91022	0.90405	0.89358	0.88188	0.87173	0.86863
	2	0.89977	0.89596	0.88984	0.87945	0.86784	0.85774	0.85462

Next, the non-dimensional first eight frequencies of the square P-FG and S-FG nanoplates with $a/h=10$ are given in Table 4. It can be seen that the power-law index and ratio of nonlocal parameters play significant effects on the frequencies of the nanoplates. The inclusion of the nonlocal parameter leads to a decrease in the frequencies of the nanoplates. Besides, the influence of the nonlocal parameters on the higher frequencies of the nanoplate is stronger than the lower frequencies. When the nonlocal parameter's ratio increases, the higher frequencies of the nanoplates decrease faster than the lower frequencies. When the power-law index is small, the frequencies of the P-FG nanoplates are higher than that of the S-FG nanoplates. When the power-law index is higher, the frequencies of the P-FG nanoplates are smaller than that of the S-FG nanoplates as demonstrated in Table 4.

Table 4. The non-dimensional first eight frequencies of the square P-FG and S-FG nanoplates

Types	k	λ	Mode 1	Mode 2	Mode 3	Mode 4	Mode 5	Mode 6	Mode 7	Mode 8
P-FG	0	0.5	1.18288	2.52699	2.52699	3.54287	4.09703	4.09703	4.79581	4.79581
		1	1.09599	2.19083	2.19083	2.95115	3.34887	3.34887	3.83728	3.83728
		1.5	1.02581	1.96082	1.96082	2.58224	2.90180	2.90180	3.29069	3.29069
		2	0.96758	1.79076	1.79076	2.32419	2.59630	2.59630	2.92625	2.92625
	1	0.5	0.96498	1.99528	1.99528	2.73969	3.13617	3.13617	3.62828	3.62828
		1	0.92569	1.85100	1.85100	2.49411	2.83074	2.83074	3.24438	3.24438
		1.5	0.89616	1.75131	1.75131	2.33194	2.63307	2.63307	3.00127	3.00127
		2	0.87185	1.67403	1.67403	2.20998	2.48632	2.48632	2.82321	2.82321
	5	0.5	0.88136	1.77332	1.77332	2.39461	2.71916	2.71916	3.11666	3.11666
		1	0.86871	1.72826	1.72826	2.31920	2.62608	2.62608	3.00064	3.00064
		1.5	0.85912	1.69501	1.69501	2.26435	2.55881	2.55881	2.91737	2.91737
		2	0.85105	1.66763	1.66763	2.21968	2.50429	2.50429	2.85022	2.85022
S-FG	0	0.5	0.99726	2.05336	2.05336	2.81275	3.21635	3.21635	3.71666	3.71666

		1	0.96133	1.92164	1.92164	2.58855	2.93740	2.93740	3.36579	3.36579
		1.5	0.92902	1.81240	1.81240	2.41062	2.72036	2.72036	3.09860	3.09860
		2	0.89977	1.71990	1.71990	2.26497	2.54526	2.54526	2.88637	2.88637
	1	0.5	0.97608	2.01242	2.01242	2.75907	3.15639	3.15639	3.64944	3.64944
		1	0.94042	1.88204	1.88204	2.53765	2.88126	2.88126	3.30396	3.30396
		1.5	0.90841	1.77410	1.77410	2.36216	2.66739	2.66739	3.04093	3.04093
		2	0.87945	1.68282	1.68282	2.21865	2.49497	2.49497	2.83207	2.83207
	5	0.5	0.95369	1.96958	1.96958	2.70342	3.09458	3.09458	3.58070	3.58070
		1	0.91822	1.84022	1.84022	2.48421	2.82257	2.82257	3.23971	3.23971
		1.5	0.88644	1.73337	1.73337	2.31085	2.61149	2.61149	2.98037	2.98037
		2	0.85774	1.64320	1.64320	2.16932	2.44156	2.44156	2.77464	2.77464

Continuously, Figure 5 shows the effects of the variation nonlocal parameter on the non-dimensional fundamental frequencies of the square P-FG and S-FG nanoplates. The dimensions of the plates are $a = b = 10\ (\mathrm{nm}^2)$, the thickness of the plates is $h = a/10$, the nonlocal parameter's ratio λ varies from 0.5 to 2. According to this figure, the variation of the nonlocal parameter has strong effects on the free vibration of the nanoplates. When the ratio of nonlocal parameters increases, the frequencies of the nanoplates decreases. In the case of P-FG nanoplates, the rate of decrease is fast when the power-law index is small, and the rate of decrease is slow when increasing the power-law index. On the other hand, the frequencies of the S-FG nanoplate decrease with a similar speed with a different value of the power-law index. It is obvious that the effects of the nonlocal parameters on the free vibration behavior of P-FG and S-FG nanoplates are different, this is completely different from other published work. The reason is that the nonlocal parameter is assumed to be constant in other published studies, so the effects of the nonlocal parameters are similar with different kinds of FG nanoplates. However, in the present model, the nonlocal parameter is assumed to vary through the thickness of the FG nanoplates as other material properties, so the influence of the nonlocal parameters depends on the power-law index and the kinds of FG nanoplates.

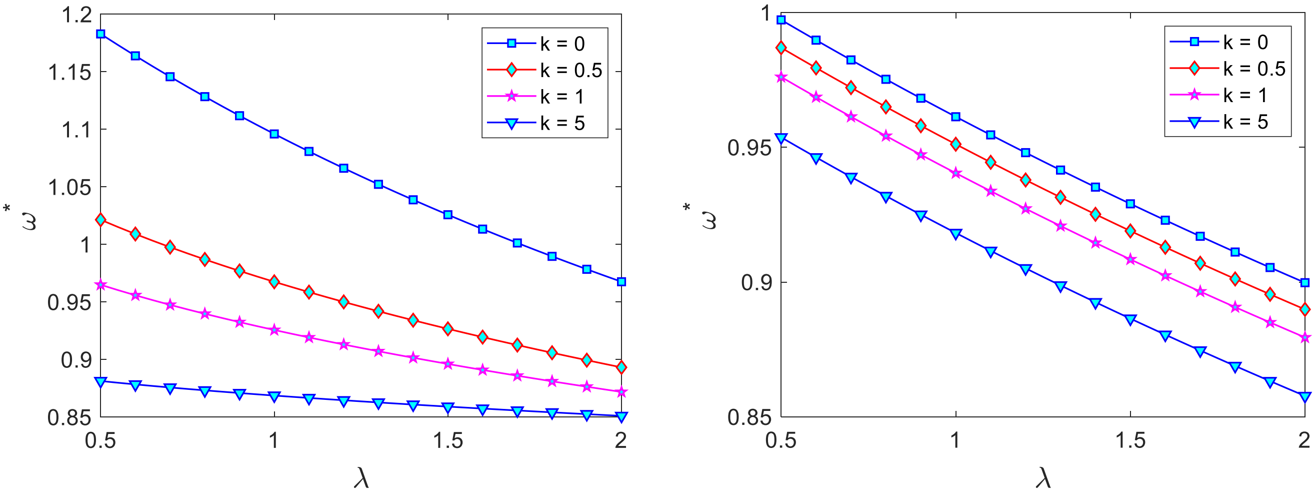

a) P-FG b) S-FG

Figure 5. The effects of the variation of the nonlocal parameter on the fundamental frequencies of the FG nanoplates

Next, the influence of the ratio of nonlocal parameters on the higher frequencies of the square P-FG and S-FG nanoplates are investigated. Figure 6 shows the variation of the non-dimensional frequencies of the P-FG and S-FG nanoplates with $a = b = 10\,(\mathrm{nm}^2)$, $h = a/10$ and $k = 2$. For both cases of P-FG and S-FG nanoplates, the frequencies of the plates decrease as the increase of nonlocal parameter's ratio. The effects of the variation of the nonlocal parameters on higher frequencies are stronger than lower frequencies. The speed of the decrease of high frequencies is faster than that of low frequencies for both P-FG and S-FG nanoplates.

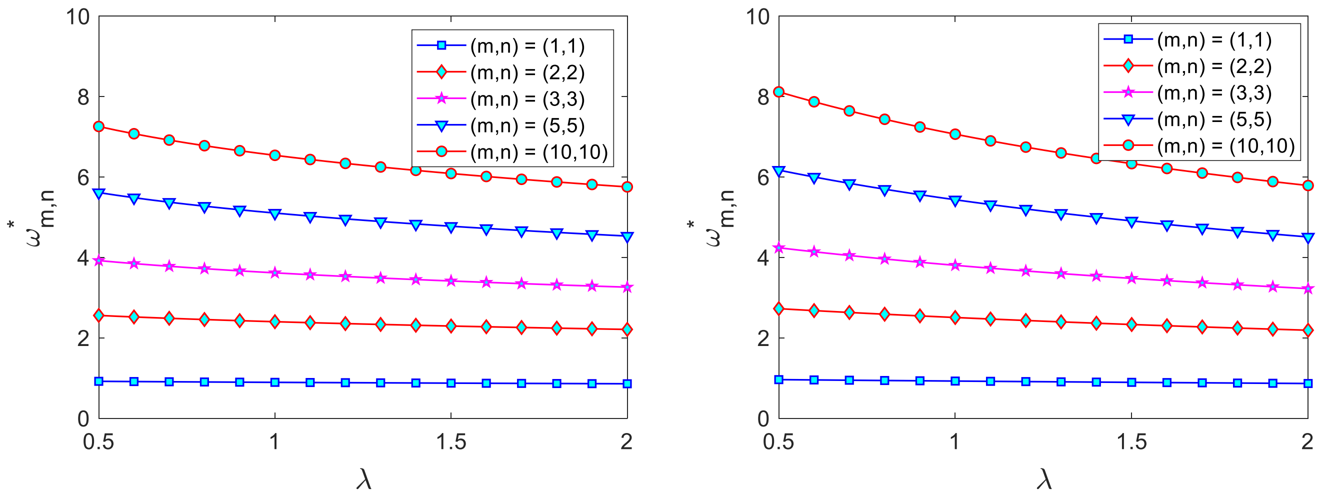

a) P-FG b) S-FG

Figure 6. The effects of the variation of the nonlocal parameter on high frequencies of the FG nanoplates

Continuously, the influence of the material parameter k on the free vibration behavior of the P-FG and S-FG nanoplates are studied. The dimensions of the plates are $a = b = 10\,(\mathrm{nm}^2)$, the thickness of the plates is $h = a/10$. Figure 7 presents the variation of the non-dimensional fundamental frequencies of the nanoplates as the functions of the material parameters. It is obvious that when the power-law index increases, the non-dimensional frequencies of the nanoplates decrease for both cases of P-FG and S-FG nanoplates. In general, the frequencies of the nanoplates decrease rapidly when the power-law index increase from 0 to 2. When the power-law index greater than 2, the frequencies of the nanoplates decrease slower. It can be seen that when the power-law index increases, the effects of the nonlocal parameter's ratio decrease in the case of P-FG nanoplates and almost unchanged with S-FG nanoplates.

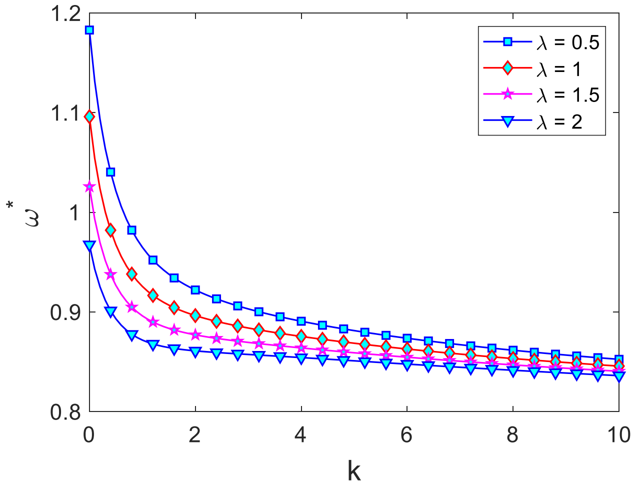

a) P-FG

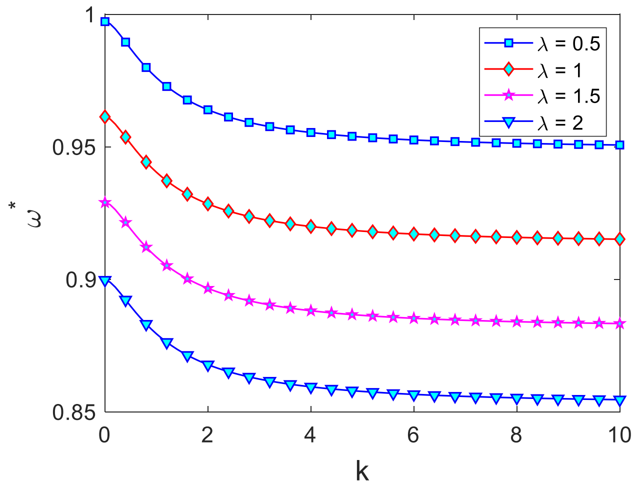

b) S-FG

Figure 7. The influence of the material parameter on the fundamental frequencies of the FG nanoplates

Figure 8 demonstrates the effects of the aspect ratio on the non-dimensional fundamental frequencies of the P-FG and S-FG nanoplates. It is noticed that the area of the plate is constant, $S = a.b = 100\,(\mathrm{nm}^2)$, it means when the length a increases, the wide b decreases, and vice versa. The thickness of the plates is $h = \sqrt{S}/10$, the power-law index is $k = 2$. It is pleasant that when the aspect ratio increases from 0.5 to 1, the non-dimensional frequencies of the P-FG and S-FG nanoplates decreases. But the non-dimensional frequencies increase when the aspect ratio increases from 1 to 2. The frequencies reach the minimum when the aspect ratio equals 1. It means the frequency of the square P-FG and S-FG nanoplate is the smallest. It can be seen that the frequency of the square plate is approximate 85% as of the rectangular one with $a/b = 0.5$ and $a/b = 2$. This minimum of the frequency of the rectangular FG nanoplates should be noticed to avoid the resonant phenomenon.

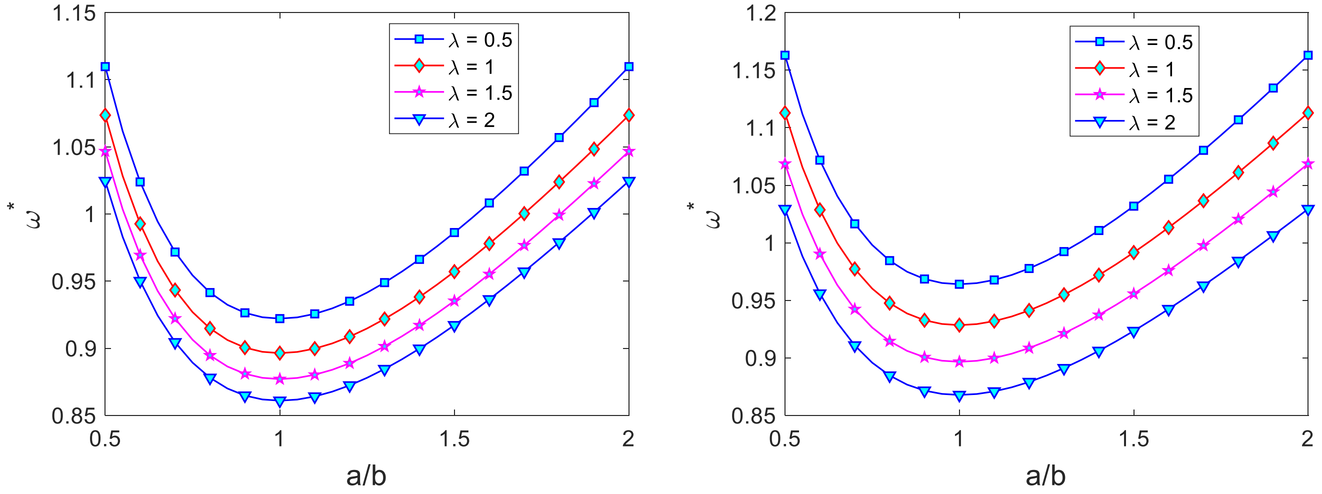

a) P-FG b) S-FG

Figure 8. The effects of the aspect ratio on the fundamental frequencies of the FG nanoplates

Lastly, the influence of the side-to-thickness ratio a/h on the non-dimensional frequencies of the P-FG and S-FG nanoplates are considered. The dimensions of the plates are $a = b = 10\ (\mathrm{nm}^2)$, the ratio of the nonlocal parameter is $\lambda = 1$. The dependence of the non-dimensional fundamental frequencies of the P-FG and S-FG nanoplates as the functions of the side-to-thickness ratio is plotted in Figure 9. The increase of the side-to-thickness ratio leads to a decrease of non-dimensional frequencies of the P-FG and S-FG nanoplates. Once again, the effects of the power-law index on the free vibration of P-FG nanoplates are stronger than that of S-FG nanoplates. It is seen that the frequency of the nanoplate with $a/h = 5$ approaches four times to that of the nanoplates with $a/h = 20$.

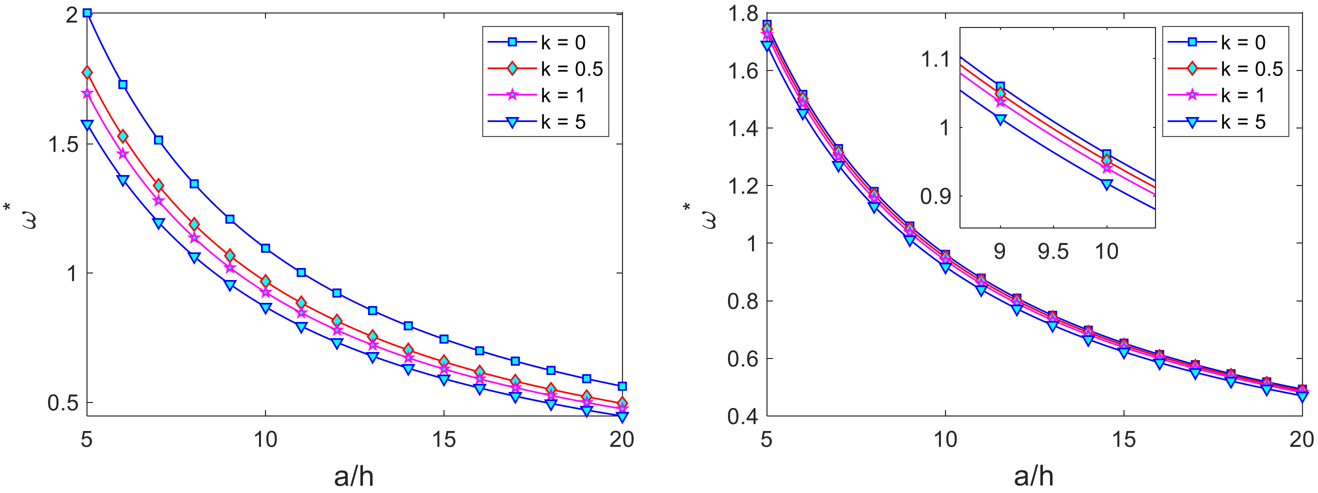

a) P-FG b) S-FG

Figure 9. The variation of the fundamental frequencies of the FG nanoplates as function of side-to-thickness ratio

4. Conclusions

In this work, the nonlocal free vibration characteristics of the P-FG and S-FG nanoplates have been investigated. The classical Eringen's nonlocal elasticity theory has been modified to take into account the variation of the nonlocal parameter through the thickness of the FG nanoplates. Some special cases of the free vibration of the FG nanoplates with constant nonlocal parameter have been considered to confirm the accuracy and correctness of the proposed algorithm. A comprehensive study on the effects of some parameter has been carried out carefully. The inclusion of the nonlocal parameter leads to reduction in the frequencies of the FG nanoplates. The numerical results showed that the variation of the nonlocal parameter plays an important role in the free vibration of the FG nanoplates, especially for higher frequencies. The effects of the nonlocal parameters not only depend on the dimensions of the nanoplates but also depend on the variation of the material components through the thickness of the FG nanoplates.

Funding

This research did not receive any specific grant from funding agencies in the public, commercial, or not-for-profit sectors.

Declaration of conflicting interests

The Author declares that there is no conflict of interest.

References

1. A.C. Eringen, Nonlocal polar elastic continua, Int. J. Eng. Sci. 10 (1972) 1–16. https://doi.org/10.1016/0020-7225(72)90070-5
2. A.C. Eringen, D.G.B. Edelen, On nonlocal elasticity, Int. J. Eng. Sci. 10 (1972) 233–248. https://doi.org/10.1016/0020-7225(72)90039-0
3. A.C. Eringen, On differential equations of nonlocal elasticity and solutions of screw dislocation and surface waves, J. Appl. Phys. 54 (1983) 4703–4710. https://doi.org/10.1063/1.332803
4. A. Rouabhia, A. Chikh, A.A. Bousahla, H. Heireche, A. Tounsi, K.H. Benrahou, A. Tounsi, M.M. Al-Zahrani, Physical stability response of a SLGS resting on viscoelastic medium using nonlocal integral first-order theory, Steel Compos. Struct. 37 (2020) 695-709. https://doi.org/10.12989/scs.2020.37.6.695
5. F. Yang, A.C.M. Chong, D.C.C. Lam, P. Tong, Couple stress based strain gradient theory for elasticity, Int. J. Solids Struct. 39 (2002) 2731–2743. https://doi.org/10.1016/S0020-7683(02)00152-X
6. S.K. Park, X.-L. Gao, Bernoulli–Euler beam model based on a modified couple stress theory, J. Micromechanics Microengineering. 16 (2006) 2355–2359. https://doi.org/10.1088/0960-1317/16/11/015
7. H.M. Ma, X.-L. Gao, J.N. Reddy, A microstructure-dependent Timoshenko beam model based on a modified couple stress theory, J. Mech. Phys. Solids. 56 (2008) 3379–3391. https://doi.org/10.1016/j.jmps.2008.09.007
8. Z. Soleimani-Javid, E. Arshid, M. Khorasani, S. Amir, A. Tounsi, Size-dependent flexoelectricity-based vibration characteristics of honeycomb sandwich plates with various boundary conditions, Adv. Nano Res. 10 (2021) 449-460. https://doi.org/10.12989/anr.2021.10.5.449
9. M. Asghari, M.H. Kahrobaiyan, M.T. Ahmadian, A nonlinear Timoshenko beam formulation based on the modified couple stress theory, Int. J. Eng. Sci. 48 (2010) 1749–1761. https://doi.org/10.1016/j.ijengsci.2010.09.025

10. N.A. Fleck, G.M. Muller, M.F. Ashby, J.W. Hutchinson, Strain gradient plasticity: Theory and experiment, Acta Metall. Mater. 42 (1994) 475–487. https://doi.org/10.1016/0956-7151(94)90502-9
11. H. Sadeghi, M. Baghani, R. Naghdabadi, Strain gradient elasticity solution for functionally graded micro-cylinders, Int. J. Eng. Sci. 50 (2012) 22–30. https://doi.org/10.1016/j.ijengsci.2011.09.006
12. C.W. Lim, G. Zhang, J.N. Reddy, A higher-order nonlocal elasticity and strain gradient theory and its applications in wave propagation, J. Mech. Phys. Solids. 78 (2015) 298–313. https://doi.org/10.1016/j.jmps.2015.02.001
13. F. Ebrahimi, M.R. Barati, A. Dabbagh, A nonlocal strain gradient theory for wave propagation analysis in temperature-dependent inhomogeneous nanoplates, Int. J. Eng. Sci. 107 (2016) 169–182. https://doi.org/10.1016/j.ijengsci.2016.07.008
14. B. Karami, M. Janghorban, A. Tounsi, On pre-stressed functionally graded anisotropic nanoshell in magnetic field, J Braz. Soc. Mech. Sci. Eng. 41 (2019) ID 495. https://doi.org/10.1007/s40430-019-1996-0
15. M.R. Barati, A general nonlocal stress-strain gradient theory for forced vibration analysis of heterogeneous porous nanoplates, Eur. J. Mech. - A/Solids. 67 (2018) 215–230. https://doi.org/10.1016/j.euromechsol.2017.09.001
16. M.N.M. Allam, A.F. Radwan, Nonlocal strain gradient theory for bending, buckling, and vibration of viscoelastic functionally graded curved nanobeam embedded in an elastic medium, Adv. Mech. Eng. 11 (2019) 1687814019837067. https://doi.org/10.1177/1687814019837067
17. H.-T. Thai, T.P. Vo, T.-K. Nguyen, S.-E. Kim, A review of continuum mechanics models for size-dependent analysis of beams and plates, Compos. Struct. 177 (2017) 196–219. https://doi.org/10.1016/j.compstruct.2017.06.040
18. A. Farajpour, M.H. Ghayesh, H. Farokhi, A review on the mechanics of nanostructures, Int. J. Eng. Sci. 133 (2018) 231–263. https://doi.org/10.1016/j.ijengsci.2018.09.006
19. S.I. Tahir, A. Chikh, A. Tounsi, M.A. Al-Osta, S.U. Al-Dulaijan, M.M. Al-Zahrani, Wave propagation analysis of a ceramic-metal functionally graded sandwich plate with different porosity distributions in

a hygro-thermal environment, Compos. Struct. 269 (2021) 114030. https://doi.org/10.1016/j.compstruct.2021.114030

20. H. Hachemi, A.A. Bousahla, A. Kaci, F. Bourada, A. Tounsi, K.H. Benrahou, A. Tounsi, M.M. Al-Zahrani, S.R. Mahmoud, Bending analysis of functionally graded plates using a new refined quasi-3D shear deformation theory and the concept of the neutral surface position, Steel Compos. Struct. 39 (2021) 51-64. https://doi.org/10.12989/scs.2021.39.1.051
21. M. Khiloun, A.A. Bousahla, A. Kaci, A. Bessaim, A. Tounsi, S.R. Mahmoud, Analytical modeling of bending and vibration of thick advanced composite plates using a four-variable quasi 3D HSDT, Eng. Comput. 36 (2020) 807-821. https://doi.org/10.1007/s00366-019-00732-1
22. A. Bakoura, F. Bourada, A.A. Bousahla, A. Tounsi, K.H. Benrahou, A. Tounsi, M.M. Al-Zahrani, S.R. Mahmoud, Buckling analysis of functionally graded plates using HSDT in conjunction with the stress function method, Comput. Concrete, 27 (2021) 73-83. https://doi.org/10.12989/cac.2021.27.1.073
23. A. Menasria, A. Kaci, A.A. Bousahla, F. Bourada, A. Tounsi, K.H. Benrahou, A. Tounsi, E.A.A. Bedia, S.R. Mahmoud, A four-unknown refined plate theory for dynamic analysis of FG-sandwich plates under various boundary conditions, Steel Compos. Struct. 36 (2020) 355-367. http://dx.doi.org/10.12989/scs.2020.36.3.355
24. S.C. Chikr, A. Kaci, A.A. Bousahla, F. Bourada, A. Tounsi, E.A.A. Bedia, S.R. Mahmoud, K.H. Benrahou, A. Tounsi, A novel four-unknown integral model for buckling response of FG sandwich plates resting on elastic foundations under various boundary conditions using Galerkin's approach, Geomechanics and Engineering, 21 (2020) 471-487. https://doi.org/10.12989/gae.2020.21.5.471
25. M.C. Rahmani, A. Kaci, A. Bousahla, F. Bourada, A. Tounsi, E.A.A. Bedia, S.R. Mahmoud, K.H. Benrahou, A. Tounsi, Influence of boundary conditions on the bending and free vibration behavior of FGM sandwich plates using a four-unknown refined integral plate theory, Comput. Concrete, 25 (2020) 225-244. https://doi.org/10.12989/cac.2020.25.3.225
26. A. Tounsi, S.U. Al-Dulaijan, M.A. Al-Osta, A. Chikh, M.M. Al-Zahrani, A. Sharif, A. Tounsi, A four variable trigonometric integral plate theory for hygro-thermo-mechanical bending analysis of AFG

ceramic-metal plates resting on a two-parameter elastic foundation, Steel Compos. Struct. 34 (2020) 511-524. http://dx.doi.org/10.12989/scs.2020.34.4.511

27. P.V. Vinh, Analysis of bi-directional functionally graded sandwich plates via higher-order shear deformation theory and finite element method, J. Sandw. Struct. Mater. 2021 ID 10996362211025811. https://doi.org/10.1177/10996362211025811
28. P.V. Vinh, N.T. Dung, N.C. Tho, D.V. Thom, L.K. Hoa, Modified single variable shear deformation plate theory for free vibration analysis of rectangular FGM plates, Structures, 29 (2021) 1435-1444. https://doi.org/10.1016/j.istruc.2020.12.027
29. P.V. Vinh, Deflections, stresses and free vibration analysis of bi-functionally graded sandwich plates resting on Pasternak's elastic foundations via a hybrid quasi-3D theory, Mech. Based Des. Struc. (2021) ID 1894948. https://doi.org/10.1080/15397734.2021.1894948
30. D.V. Thom, P.V. Vinh, N.H. Nam, On the Development of Refined Plate Theory for Static Bending Behavior of Functionally Graded Plates, Math. Probl. Eng. 2020 (2020) ID 2836763. https://doi.org/10.1155/2020/2836763
31. P.V. Vinh, L.Q. Huy, Finite element analysis of functionally graded sandwich plates with porosity via a new hyperbolic shear deformation theory, Def. Technol. (2021). https://doi.org/10.1016/j.dt.2021.03.006
32. P.V. Vinh, Formulation of a New Mixed Four-Node Quadrilateral Element for Static Bending Analysis of Variable Thickness Functionally Graded Material Plates, Math. Probl. Eng. 2021 (2021) ID 6653350. https://doi.org/10.1155/2021/6653350
33. Y.Q. Zhang, G.R. Liu, J.S. Wang, Small-scale effects on buckling of multiwalled carbon nanotubes under axial compression, Phys. Rev. B. 70 (2004) 205430. https://doi.org/10.1103/PhysRevB.70.205430
34. Y.-G. Hu, K.M. Liew, Q. Wang, X.Q. He, B.I. Yakobson, Nonlocal shell model for elastic wave propagation in single- and double-walled carbon nanotubes, J. Mech. Phys. Solids. 56 (2008) 3475–3485. https://doi.org/10.1016/j.jmps.2008.08.010

35. M. Bellal, H. Hebali, H. Heireche, A. Bousahla, A. Tounsi, F. Bourada, S.R. Mahmoud, E.A.A. Bedia, A. Tounsi, Buckling behavior of a single-layered graphene sheet resting on viscoelastic medium via nonlocal four-unknown integral model, Steel Compos. Struct. 34 (2020) 643-655. https://doi.org/10.12989/scs.2020.34.5.643. https://doi.org/10.12989/anr.2019.7.6.431
36. M. Hussain, M.N. Naeem, A. Tounsi, M. Taj, Nonlocal effect on the vibration of armchair and zigzag SWCNTs with bending rigidity, Adv. Nano Res. 7 (2019) 431-442. https://doi.org/10.12989/anr.2019.7.6.431
37. S. Asghar, M.N. Naeem, M. Husain, M. Taj, A. Tounsi, Prediction and assessment of nonlocal natural frequencies of DWCNTs: Vibration analysis, Comput. Concrete, 25 (2020) 133-144. https://doi.org/10.12989/cac.2020.25.2.133
38. R. Li, G.A. Kardomateas, Vibration Characteristics of Multiwalled Carbon Nanotubes Embedded in Elastic Media by a Nonlocal Elastic Shell Model, J. Appl. Mech. 74 (2007) 1087–1094. https://doi.org/10.1115/1.2722305
39. Q. Wang, V.K. Varadan, Application of nonlocal elastic shell theory in wave propagation analysis of carbon nanotubes, Smart Mater. Struct. 16 (2007) 178–190. https://doi.org/10.1088/0964-1726/16/1/022
40. H. Rouhi, R. Ansari, Nonlocal analytical Flugge shell model for axial buckling of double-walled carbon nanotubes with different end conditions, Nano. 07 (2012) 1250018. https://doi.org/10.1142/S179329201250018X
41. H. Matouk, A. Bousahla, H. Heireche, F. Bourada, E.A.A. Bedia, A. Tounsi, S.R. Mahmoud, K.H. Benrahou, Investigation on hygro-thermal vibration of P-FG and symmetric S-FG nanobeam using integral Timoshenko beam theory, Adv. Nano Res. 8 (2020) 293-305. https://doi.org/10.12989/anr.2020.8.4.293
42. P. Lu, P.Q. Zhang, H.P. Lee, C.M. Wang, J.N. Reddy, Non-local elastic plate theories, Proc. R. Soc. A Math. Phys. Eng. Sci. 463 (2007) 3225–3240. https://doi.org/10.1098/rspa.2007.1903

43. S.C. Pradhan, J.K. Phadikar, Small scale effect on vibration of embedded multilayered graphene sheets based on nonlocal continuum models, Phys. Lett. A. 373 (2009) 1062–1069. https://doi.org/10.1016/j.physleta.2009.01.030
44. T. Aksencer, M. Aydogdu, Levy type solution method for vibration and buckling of nanoplates using nonlocal elasticity theory, Phys. E Low-Dimensional Syst. Nanostructures. 43 (2011) 954–959. https://doi.org/10.1016/j.physe.2010.11.024
45. Z.-B. Shen, H.-L. Tang, D.-K. Li, G.-J. Tang, Vibration of single-layered graphene sheet-based nanomechanical sensor via nonlocal Kirchhoff plate theory, Comput. Mater. Sci. 61 (2012) 200–205. https://doi.org/10.1016/j.commatsci.2012.04.003
46. Y. Zhang, Z.X. Lei, L.W. Zhang, K.M. Liew, J.L. Yu, Nonlocal continuum model for vibration of single-layered graphene sheets based on the element-free kp-Ritz method, Eng. Anal. Bound. Elem. 56 (2015) 90–97. https://doi.org/10.1016/j.enganabound.2015.01.020
47. Y. Zhang, L.W. Zhang, K.M. Liew, J.L. Yu, Buckling analysis of graphene sheets embedded in an elastic medium based on the kp-Ritz method and non-local elasticity theory, Eng. Anal. Bound. Elem. 70 (2016) 31–39. https://doi.org/10.1016/j.enganabound.2016.05.009
48. R. Ansari, S. Sahmani, B. Arash, Nonlocal plate model for free vibrations of single-layered graphene sheets, Phys. Lett. A. 375 (2010) 53–62. https://doi.org/10.1016/j.physleta.2010.10.028
49. R. Ansari, B. Arash, H. Rouhi, Vibration characteristics of embedded multi-layered graphene sheets with different boundary conditions via nonlocal elasticity, Compos. Struct. 93 (2011) 2419–2429. https://doi.org/10.1016/j.compstruct.2011.04.006
50. S. Hosseini-Hashemi, M. Bedroud, R. Nazemnezhad, An exact analytical solution for free vibration of functionally graded circular/annular Mindlin nanoplates via nonlocal elasticity, Compos. Struct. 103 (2013) 108–118. https://doi.org/10.1016/j.compstruct.2013.02.022
51. A. Anjomshoa, M. Tahani, Vibration analysis of orthotropic circular and elliptical nano-plates embedded in elastic medium based on nonlocal Mindlin plate theory and using Galerkin method, J. Mech. Sci. Technol. 30 (2016) 2463–2474. https://doi.org/10.1007/s12206-016-0506-x

52. M. Balubaid, A. Tounsi, B. Dakhel, S.R. Mahmoud, Free vibration investigation of FG nanoscale plate using nonlocal two variables integral refined plate theory, Comput. Concrete, 24 (2019) 579-586. http://dx.doi.org/10.12989/cac.2019.24.6.579

53. B. Fatima, B.K. Halim, B. Ismahene, T. Abdelouahed, A nonlocal zeroth-order shear deformation theory for free vibration of functionally graded nanoscale plates resting on elastic foundation, Steel Compos. Struct. 20 (2016) 227–249. https://doi.org/10.12989/SCS.2016.20.2.227

54. L.K. Hoa, P.V. Vinh, N.D. Duc, N.T. Trung, L.T. Son, D.V. Thom, Bending and free vibration analyses of functionally graded material nanoplates via a novel nonlocal single variable shear deformation plate theory, P. I. Mech. Eng. C-J Mec. 2020 ID 0954406220964522. https://doi.org/10.1177/0954406220964522

55. A.M. Zenkour, Nonlocal elasticity and shear deformation effects on thermal buckling of a CNT embedded in a viscoelastic medium, Eur. Phys. J. Plus. 133 (2018) 196. https://doi.org/10.1140/epjp/i2018-12014-2

56. A.M. Zenkour, A.F. Radwan, Nonlocal mixed variational formula for orthotropic nanoplates resting on elastic foundations, Eur. Phys. J. Plus. 135 (2020) 493. https://doi.org/10.1140/epjp/s13360-020-00504-7

57. A.M. Zenkour, Z.S. Hafed, A.F. Radwan, Bending Analysis of Functionally Graded Nanoscale Plates by Using Nonlocal Mixed Variational Formula, Mathematics. 8 (2020). https://doi.org/10.3390/math8071162

58. R. Aghababaei, J.N. Reddy, Nonlocal third-order shear deformation plate theory with application to bending and vibration of plates, J. Sound Vib. 326 (2009) 277–289. https://doi.org/10.1016/j.jsv.2009.04.044

59. R. Ansari, S. Sahmani, Prediction of biaxial buckling behavior of single-layered graphene sheets based on nonlocal plate models and molecular dynamics simulations, Appl. Math. Model. 37 (2013) 7338–7351. https://doi.org/10.1016/j.apm.2013.03.004

60. S. Hosseini-Hashemi, M. Kermajani, R. Nazemnezhad, An analytical study on the buckling and free vibration of rectangular nanoplates using nonlocal third-order shear deformation plate theory, Eur. J. Mech. - A/Solids. 51 (2015) 29–43. https://doi.org/10.1016/j.euromechsol.2014.11.005
61. A. Daneshmehr, A. Rajabpoor, M. Pourdavood, Stability of size dependent functionally graded nanoplate based on nonlocal elasticity and higher order plate theories and different boundary conditions, Int. J. Eng. Sci. 82 (2014) 84–100. https://doi.org/10.1016/j.ijengsci.2014.04.017
62. A. Daneshmehr, A. Rajabpoor, A. Hadi, Size dependent free vibration analysis of nanoplates made of functionally graded materials based on nonlocal elasticity theory with high order theories, Int. J. Eng. Sci. 95 (2015) 23–35. https://doi.org/10.1016/j.ijengsci.2015.05.011
63. P. Malekzadeh, M. Shojaee, Free vibration of nanoplates based on a nonlocal two-variable refined plate theory, Compos. Struct. 95 (2013) 443–452. https://doi.org/10.1016/j.compstruct.2012.07.006
64. S. Narendar, Buckling analysis of micro-/nano-scale plates based on two-variable refined plate theory incorporating nonlocal scale effects, Compos. Struct. 93 (2011) 3093–3103. https://doi.org/10.1016/j.compstruct.2011.06.028
65. S. Narendar, S. Gopalakrishnan, Scale effects on buckling analysis of orthotropic nanoplates based on nonlocal two-variable refined plate theory, Acta Mech. 223 (2012) 395–413. https://doi.org/10.1007/s00707-011-0560-5
66. M. Sobhy, Generalized two-variable plate theory for multi-layered graphene sheets with arbitrary boundary conditions, Acta Mech. 225 (2014) 2521–2538. https://doi.org/10.1007/s00707-014-1093-5
67. M. Sobhy, Levy-type solution for bending of single-layered graphene sheets in thermal environment using the two-variable plate theory, Int. J. Mech. Sci. 90 (2015) 171–178. https://doi.org/10.1016/j.ijmecsci.2014.11.014
68. M. Sobhy, Hygrothermal vibration of orthotropic double-layered graphene sheets embedded in an elastic medium using the two-variable plate theory, Appl. Math. Model. 40 (2016) 85–99. https://doi.org/10.1016/j.apm.2015.04.037

69. M. Sobhy, Hygrothermal deformation of orthotropic nanoplates based on the state-space concept, Compos. Part B Eng. 79 (2015) 224–235. https://doi.org/10.1016/j.compositesb.2015.04.042
70. M. Sobhy, A.M. Zenkour, Nonlocal Thermal and Mechanical Buckling of Nonlinear Orthotropic Viscoelastic Nanoplates Embedded in a Visco-Pasternak Medium, Int. J. Appl. Mech. 10 (2018) 1850086. https://doi.org/10.1142/S1758825118500862
71. A.M. Zenkour, M. Sobhy, Nonlocal elasticity theory for thermal buckling of nanoplates lying on Winkler–Pasternak elastic substrate medium, Phys. E Low-Dimensional Syst. Nanostructures. 53 (2013) 251–259. https://doi.org/10.1016/j.physe.2013.04.022
72. H.-T. Thai, T.P. Vo, T.-K. Nguyen, J. Lee, 44. A nonlocal sinusoidal plate model for micro/nanoscale plates, Proc. Inst. Mech. Eng. Part C J. Mech. Eng. Sci. 228 (2014) 2652–2660. https://doi.org/10.1177/0954406214521391
73. A. Bessaim, M.S.A. Houari, F. Bernard, A. Tounsi, A nonlocal quasi-3D trigonometric plate model for free vibration behaviour of micro/nanoscale plates, Struct. Eng. Mech. 56 (2015) 223–240. https://doi.org/10.12989/SEM.2015.56.2.223
74. M. Sobhy, A.F. Radwan, A New Quasi 3D Nonlocal Plate Theory for Vibration and Buckling of FGM Nanoplates, Int. J. Appl. Mech. 09 (2017) 1750008. https://doi.org/10.1142/S1758825117500089
75. P.V. Vinh, L.Q. Huy, Influence of variable nonlocal parameter and porosity on the free vibration behavior of functionally graded nanoplates, Shock Vib. 2021 (2021) 1219429. https://doi.org/10.1155/2021/1219429
76. P. Van Vinh, A. Tounsi, The role of spatial variation of the nonlocal parameter on the free vibration of functionally graded sandwich nanoplates, Eng. Comput. (2021). https://doi.org/10.1007/s00366-021-01475-8
77. R.C. Batra, Misuse of Eringen's nonlocal elasticity theory for functionally graded materials, Int. J. Eng. Sci. 159 (2021) 103425. https://doi.org/10.1016/j.ijengsci.2020.103425